INDEX COPERNICUS INTERNATIONAL

ORYGINAL ARTICLE

Estimation of ethmoid roof depth and length of lateral lamella of the cribriform plate, upper attachment of the uncinate process and anterior ethmoid artery in multiplanar reconstructions of Computed Tomography

Greta Berger[1], Vitaly Grinevych[1], Anna Justyna Milewska[2], Adam Lukasiewicz[1], Eugeniusz Tarasow[1]

[1]TMS Diagnostyka, Bialystok, Poland; Head: prof. Eugeniusz Tarasow MD PhD
[2]Department of Medical Informatics and Statistics, Medical University of Bialystok, Poland

Article history: Received: 29.03.2020 Accepted: 23.06.2020 Published: 24.06.2020

ABSTRACT:

Objectives: The aim is to assess the relationship of the anterior ethmoid artery with the upper attachment of the uncinate process and their relation with the lateral lamella of the cribriform plate in multiplanar reconstructions (i.e. coronal, axial and sagittal) of Computed Tomography. We measured the depth of the olfactory fossa, the length of the LLCP and determined the most superior attachment of the uncinate process, which designates boundaries of the frontal recess anteriorly, laterally and medially [4, 6].

Methods: All CT examinations were performed with the 320-detector *Aquilion ONE CT scanner* (Canon Medical Systems, Otawara, Japan). Axial, coronal, sagittal reconstruction were performed with dedicated workstation software (Vitrea Enterprise Suite, version 6.7; Vital images, Minnetonka USA). The Statistica13 software was used for analysis and the results were considered statistically significant at the level of $P < 0.05$.

Results: The most frequent types of UP according to Landsberg-Friedman criteria in the group of men are: type I – 30.77%, type II – 30.77%, type III – 26.92%, type VI – 7.69%, type V – 3.85%, type IV – 0%. In women's group: type III – 44.12%, type II – 32.35%, type I – 8.82%, type V – 8.82%, type IV – 5.88%, type VI – 0%. The median LLCP length in the anterior-posterior dimension is 13 mm i.e. Yenigun type II on both sides. The median value of depth in the superior-inferior dimension of LLCP in the ethmoid roof is 5 mm i.e. Keros type II on both sides. The mean distance between AEA and UAUP is approximately 9.73 mm and 9.16 mm on the right and left side respectively.

Conclusions: The assessment of AEA,UAUP and configuration of the anterior skull base in CT multiplanar reconstructions contributes to optimizing the results of frontal sinus surgery.

KEYWORDS: anterior ethmoid artery, computed tomography, lateral lamella of the cribriform plate, multiplanar reconstructions, uncinate process

ABBREVIATIONS

AET – anterior ethmoid artery
CSF – cerebrospinal fluid
CT – computed tomography
LLCP – lateral lamella of the cribriform plate
MPR – multiplanar reconstructions
UAUP – upper attachment of the uncinate process
UP – uncinate process

INTRODUCTION

Approach to the frontal sinus ostium is preceded by the removal of the most superior part of the uncinate process [1]. In the case of anterior skull base configuration i.e. Keros type III, Yenigun type III, surgical dissection medially towards the upper attachment of the uncinate process (UAUP) may cause fracture in the lateral lamella of the cribriform plate (LLCP). This may result in unintended cerebrospinal fluid (CSF) leak. Furthermore, the increased length and slant of the lateral lamella of the cribriform plate (LLCP) increase the probability of CSF leak during surgical manipulations. Moreover, bleeding from the anterior ethmoid artery (AEA) poses an additional risk from surgical point of view, as it impedes visualization of the frontal region. AEA traverses at variable distances from the ethmoid roof, then transfixes LLCP and enters the olfactory fossa. For that reason, particular attention has to be given to UAUP removal as this anatomical structure is placed anteriorly to the frontal recess [2]. Negligence in UAUP removal may also impede natural function of the frontal sinus. Indeed, understanding the physiology around the frontal sinus yields better results in operations of the frontal region. Messerklinger et al. [3] was the first to stress that the frontal sinus is unique in that it expresses a recirculation phenomenon. The mucus shifts along the lateral side of the sinus and turns medially over the sinus floor and down the lateral frontal recess wall. As much as 60% of parietal mucosa secretions are directed to the frontal cavity as they reach the frontal recess [3, 4]. The use of preoperative multiplanar reconstructions (MPR) in CT yields exactitude in proper estimation of the frontal region [5]. Radiological landmarks of AEA are e.g. ethmoid sulcus on the vertical portion of the cribriform plate and ethmoidal notch on the medial orbital wall [6].

METHODS

Computed Tomography (CT) investigations, performed at TMS Diagnostyka (Bialystok, Poland) between 2019 and 2020, were retrospectively surveyed.

Tab. I. Statistical analysis. The results were considered statistically significant at the level of p < 0,05.

VARIABLE	N	MEAN (MM)	MEDIANA (MM)	MINIMUM (MM)	MAXIMUM (MM)	LOWER QUARTILE	UPPER QUARTILE
Keros right	60	5,13	5,00	1,00	11,00	4,00	7,00
Keros left	60	5,17	5,00	1,00	11,00	3,00	6,50
Yenigun right	60	12,95	13,00	6,00	20,00	11,00	15,00
Yenigun left	60	13,13	13,00	3,00	20,00	12,00	15,00
Age	60	43,62	41,00	18,00	82,00	33,00	52,00
AEAUAUP right	60	9,73	10,00	2,00	15,00	8,00	13,00
AEAUAUP left	60	9,17	9,50	2,00	15,00	7,00	11,00

Tab. II. Statistical analysis correlated to age and sex.

VARIABLE	SEX	N	MEAN (MM)	MEDIANA (MM)	MINIMUM (MM)	MAXIMUM (MM)	LOWER QUARTILE	UPPER QUARTILE
Keros right	men	26	5,84	6,00	1,00	11,00	4,00	7,00
Keros right	men	26	5,96	6,00	2,00	11,00	5,00	8,00
Yenigun right	men	26	12,69	12,50	9,00	18,00	11,00	15,00
Yenigun right	men	26	12,73	12,00	8,00	19,00	11,00	15,00
Age	men	26	36,38	35,00	18,00	60,00	27,00	45,00
AEA-UAUP right	men	26	8,96	8,00	4,00	14,00	6,00	12,00
AEA-UAUP right	men	26	8,96	9,50	2,00	14,00	7,00	11,00
Keros right	women	34	4,59	4,50	1,00	8,00	4,00	6,00
Keros left	women	34	4,56	4,00	1,00	9,00	3,00	6,00
Yenigun right	women	34	13,15	13,50	6,00	20,00	11,00	15,00
Yenigun left	women	34	13,44	13,00	3,00	20,00	12,00	15,00
Age	women	34	49,15	45,00	26,00	82,00	39,00	62,00
AEA-UAUP right	women	34	10,32	10,00	2,00	15,00	9,00	13,00
AEA-UAUP left	women	34	9,32	9,50	4,00	15,00	7,00	11,00

All CT examinations were performed using the 320-detector *Aquilion ONE CT scanner* (Canon Medical Systems, Otawara, Japan). For all examinations, unenhanced volume CT was routinely performed in the supine position, without gantry tilt, in axial planes, parallel to the hard palate. The scanning length covered the cranium from the frontal sinus to the mandible. The CT data acquisition was performed using volume, single rotation scan with the following technical parameters: 120 kV, 150 mA, 75 effective mAs, 0.5 second rotation time, section thickness of 0.5 mm, a field of view (FOV) of 220 mm².

All data sets were reconstructed with separate kernels for the bone and soft tissue. Axial, coronal and sagittal reconstruction were performed by using dedicated workstation software (Vitrea Enterprise Suite, version 6. 7; Vital images, Minnetonka USA).

All sixty patients, mean age 43 years (i.e. males 26 years, females 34 years), had computed tomography (CT) using multiplanar reconstructions (axial, coronal, sagittal). All of those who met the inclusion criteria (i.e. no evidence of congenital either acquired deformities of the skull base and paranasal sinuses, negative history of previous

Tab. III. Upper attachment of the uncinate process according to Landsberg- Friedman criteria between the gender (twenty-six men and thirty-four woman). The most frequent type of the uncinate process between men i.e. type I and II and woman i.e. type III and II.

GENDER	LANDSBERG-FRIEDMAN TYPE I (superior attachment to the lamina papyracea)	LANDSBERG-FRIEDMAN TYPE II (superior attachment to the posteromedial wall of ager nasi cell)	LANDSBERG-FRIEDMAN TYPE III (superior attachment to the connection between the middle turbinate and lateral lamella of the cribriform plate)	LANDSBERG-FRIEDMAN TYPE IV (superior attachment to the skull base)	LANDSBERG-FRIEDMAN TYPE V (superior attachment to the middle turbinate)	LANDSBERG-FRIEDMAN TYPE VI (superior attachment to the lamina papyracea and the connection between the middle turbinate and lateral lamella of the cribriform plate)
Men	8 (30,77 %)	8 (30,77 %)	7 (26,92 %)	0 (0,00%)	1 (3,85 %)	2 (7,69 %)
Women	3 (8,82%)	11 (32,35 %)	15 (44,12 %)	2 (5,88%)	3 (8,82%)	0 (0,00%)

Tab. IV. Distinction between upper attachment of the uncinate process (according to Landsberg-Friedman criteria) and distance amongst anterior ethmoid artery and upper attachment of the uncinate process on the right and left side respectively. Because of the small number of patients expressing uncinate process type IV, V and VI, we decided to create one group for statistical analysis.

VARIABLE	UNCINATE PROCESS LANDSBERG-FRIEDMAN TYPE	N	MEAN (MM)	MEDIANA (MM)	MINIMUM (MM)	MAXIMUM (MM)	LOWER QUARTILE	UPPER QUARTILE
AEA-UAUP right	I	11	9,36	8,00	4,00	14,00	7,00	13,00
AEA-UAUP right	II	19	9,36	9,00	2,00	14,00	6,00	13,00
AEA-UAUP right	III	22	11,04	11,00 *	6,00	15,00	9,00	13,00
AEA-UAUP right	IV–VI	8	7,50	8,00*	4,00	10,00	6,50	8,50
AEA-UAUP left	I	15	8,53	9,00	2,00	13,00	6,00	11,00
AEA-UAUP left	II	19	9,21	10,00	4,00	14,00	8,00	12,00
AEA-UAUP left	III	15	9,60	10,00	6,00	13,00	8,00	11,00
AEA-UAUP left	IV–VI	11	9,36	9,00	6,00	15,00	7,00	11,00

* There is statistically significant difference between type III and group IV-VI for the right side ($p = 0,017$).

sinus surgery or trauma, age > 18 years at the time of imaging) were recruited to the study. The exclusion criteria were as follows: apoplastic paranasal sinuses, extensive rhinosinusitis with polyposis, previous history of facial trauma and sinus surgery). All personal data of the patients were anonymized.

The findings from the CT scans were reviewed and interpreted by two independent specialists – a laryngologist (G. Berger) and a radiologist (V. Grinevych). In the study, Keros criteria were applied, i.e. assessment of LLCP depth in the ethmoid roof (type 1: 0–3 mm; type 2: 4–7 mm; type 3: 8–16 mm) [7] and Yenigun criteria were used to estimate the dimension of the anterior-posterior length of LLCP (type 1: 6–10 mm; type 2: 11–15 mm; type 3: 16–20 mm) [8]. In multiplanar reconstructions of CT, in axial scans, the anterior-posterior dimension of LLCP was assessed between AEA and anteriorly to the border of the crista galli.

We analyzed associations between the anterior skull base configuration (Keros and Yenigun criteria) with trajectory of the anterior ethmoid artery (AEA) and upper attachment of the uncinate process (UAUP).

Measurements included:

1. upper attachment of the uncinate process (UAUP) according to Landsberg and Friedman [9] criteria (in the coronal and sagittal planes);
2. LLCP length in the anterior-posterior dimension, according to the Yenigun criteria (axial scans) [8];
3. Depth in the superior-inferior dimension of the lateral lamella of the cribriform plate (LLCP) in the ethmoid roof according to Keros criteria (coronal scans) [7];
4. Distance between the anterior ethmoid artery (AET) and the upper attachment of the uncinate process (UAUP) (sagittal scans). The point at which the upper attachment of the uncinate process became horizontal to the anterior skull base was the reference point in the measurement of the distance between AEA and UAUP.

STATISTICAL ANALYSIS

The Statistica 13 (TIBCO Software Inc.) software was used for statistical analysis. The Mann-Whitney U test was applied to determine differences between groups and the non-parametric ANOVA Kruscal-Wallis rank test with the post-hoc test for multiple comparisons of average ranks for all trials were used in the case of multiple groups. To analyze the strength of the correlations between the quantitative variables, Spearman's rank correlation coefficients were calculated. The results were considered statistically significant at the level of $p < 0.05$.

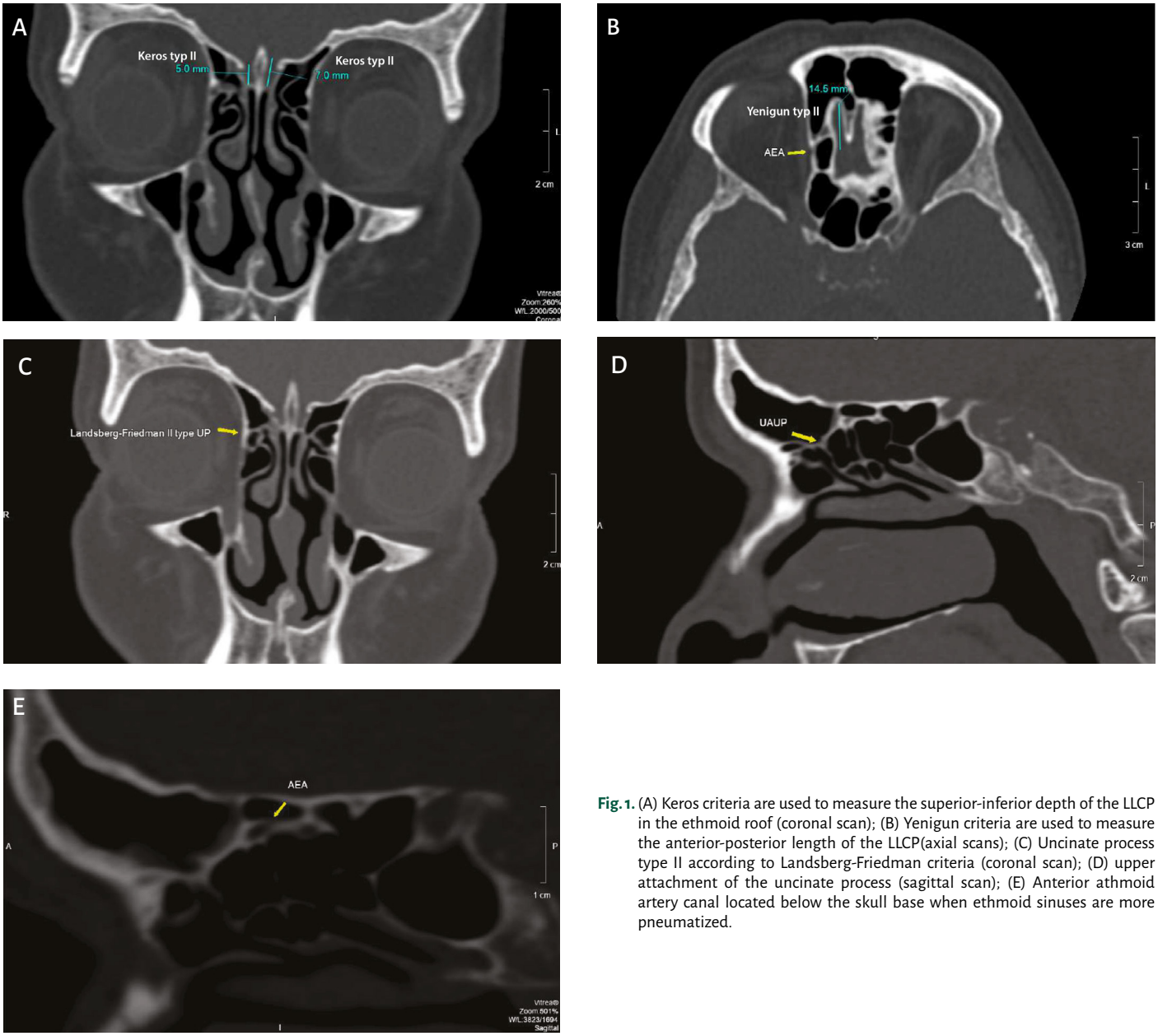

Fig. 1. (A) Keros criteria are used to measure the superior-inferior depth of the LLCP in the ethmoid roof (coronal scan); (B) Yenigun criteria are used to measure the anterior-posterior length of the LLCP(axial scans); (C) Uncinate process type II according to Landsberg-Friedman criteria (coronal scan); (D) upper attachment of the uncinate process (sagittal scan); (E) Anterior athmoid artery canal located below the skull base when ethmoid sinuses are more pneumatized.

RESULTS

1. The most frequent types of UP according to Landberg-Friedman criteria in the group of twenty-six (26) men are as follows: type I – 30.77%, type II – 30.77%, type III – 26.92%, type VI – 7.69%, type V – 3.85%, type IV – 0%. In the group of women: type III – 44.12%, type II – 32.35%, type I – 8.82%, type V – 8.82%, type IV – 5.88%, type VI – 0.00%;
2. The median LLCP length in the anterior-posterior dimension, according to Yenigun criteria, is 13 mm (range from 6 to 20 mm) on the right side, which accounts for type II Yenigun. On the left side, the median LLCP length is 13 mm (range from 3 to 20 mm), i.e. type II Yenigun;
3. The median value of depth in the superior-inferior dimension of the LLCP in the ethmoid roof according to Keros criteria is 5 mm (range from 1 to 11 mm), i.e. type II Keros on the right and left side;
4. The distance between AEA and UAUP was approximately 9.73 mm (range from 2 to 15 mm) on the right side and 9.16 mm (range from 2 to 10 mm) on the left side.

DISCUSSION

AEA derives from the ophthalmic artery, passes in the orbit between the medial rectus and the superior oblique muscle. When AEA leaves the orbit, it traverses the ethmoid roof, gives off branches to the nasal fossa and the superior part of the septum. The last branch of AEA, after it enters the olfactory fossa, is the anterior meningeal artery [6]. Though rarely, AEA may be a source of epistaxis as well as sphenopalatine artery or facial artery [10]. Bischoff et al. [11] recommend ligation of AEA by an external approach in case of posterior, non-sphenopalatine artery epistaxis. However, Turri-Zanoni et al. [12] have proved that direct coagulation of the septal branches of AEA by using bipolar forceps and endoscopic endonasal approach is effective and does not always require dissection of the main AEA's trunk. It is worth to note that both AEA ligation by an external approach and embolization bring about a high risk of post-operative complications, e.g. diplopia or ophthalmic artery disfunction respectively [13]. In functional endoscopic sinus surgery (FESS), intraoperative identification of the AEA trajectory is not recommended but if AEA is preoperatively

Tab. V. Anterior skull base configuration according to Keros and Yenigun criteria. The most frequent type between women and men is type II in Keros (superior-inferior dimension) as well as in Yenigun (anterior-posterior dimension) criteria on the both sides.

		WOMEN (N=34)	MEN (N=26)
Keros Right	I (0–3 mm)	8 (23,53%)	6 (23,08%)
	II (4–7 mm)	25 (73,53%)	14 (53,85%)
	III (8–16 mm)	1 (2,94%)	6 (23,08%)
Keros Left	I (0–3 mm)	10 (29,41%)	6 (23,08%)
	II (4–7 mm)	23 (67,65%)	13 (50,00%)
	III (8–16 mm)	1 (2,94%)	7 (26,92%)
Yenigun Right	I (6–10 mm)	6 (17,65%)	6 (23,08%)
	II (11–15 mm)	20 (58,82%)	17 (65,38%)
	III (16–20 mm)	8 (23,53%)	3 (11,54%)
Yenigun Left	I (6–10 mm)	3 (8,82%)	5 (19,23%)
	II (11–15 mm)	24 (70,59%)	19 (73,08%)
	III (16–20 mm)	7 (20,59%)	2 (7,69%)

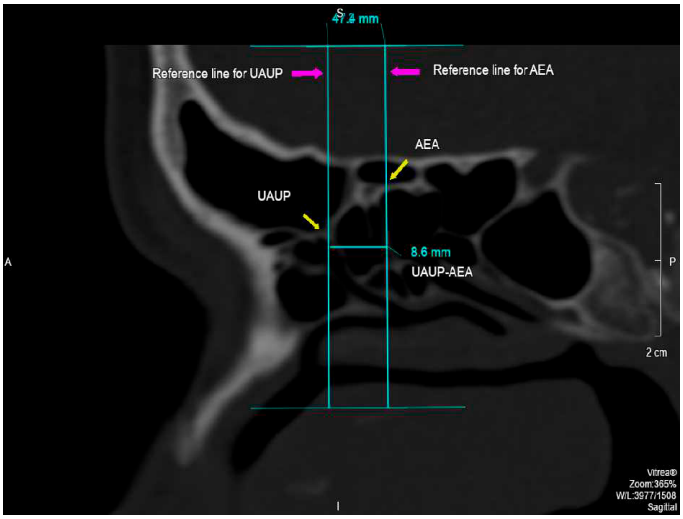

Fig. 2. Distance between upper attachment of the uncinate process and anterior ethmoid artery.

thoroughly assessed on radiological imaging and encountered during surgery, the injuries should be prevented by all means. According to Moon et al. [14] and Simmen et al. [15], the AEA canal is located between the second and the third lamella in most cases. With regard to authors mentioned above, we found preponderance of AEA location between the bulla lamella and the basal lamella of the middle turbinate in sagittal planes of CT. Contrary to Moon et al. [14] and Simmen et al. [15], Ferrari et al. [16] revealed the prevalence of AEA's location within the third lamella and less frequently anteriorly to the basal lamella of the middle turbinate. Ferrari et al. [16] explain that AEA cannot be exposed without entire excavation of the anterior wall of the bulla ethmoidalis. Heinz Stammberger asserts that AEA is encountered 1–2 mm behind the anterior wall of the bulla ethmoidalis, just behind the first fovea of the ethmoid roof [17]. In addition to this, Minni et al. [18] stress that AEA may be within the suprabullar cells (i.e. the posterior group of cells in the frontal recess, located above the bulla ethmoidalis and below the posterior wall of the frontal recess), especially when suprabullar cells coexist with supraorbital cells. To quote Simmen et al. [19], when ethmoid sinuses are more pneumatized, AEA is suspended below the skull base. On the contrary, a low level of ethmoid sinuses and skull base pneumatization correlates with AEA position within the skull base. Nevertheless, the knowledge of AEA anatomy is vital in the FESS procedure, but as Turri-Zanoni et al. [12] emphasize, also septal branches of AEA are a crucial landmark in Draf type III sinusotomy. To identify the posterior wall of the frontal sinus, septal branches of AEA represent the limit to which the superior portion of the nasal septum and the frontal sinus floor can be drilled out.

Turri-Zanoni et al. [12] highlight that septal AEA branches delineate the posterior border of Draf type III sinusotomy, which enables a decrease in iatrogenic CSF leak during enlargement of frontal median drainage.

The superior attachment of the uncinate process is recommended as a landmark and it indicates the trajectory of frontal sinus drainage [1]. When an unremoved remnant of UAUP remains by the ostium, either recess of the frontal sinus, postoperative narrowing and patency impairment may occur. Thereby, the preoperative assessment of UAUP on coronal and sagittal CT scans guides the surgeon. According to the "uncapping the egg" technique inferred by Heinz Stammberger [19], another reason for recurring postoperative frontal sinus problems may be an unremoved bony "eggshell" in the frontal recess.

Our findings imply that UAUP (according to Landsberg and Friedman criteria) [9] is not only a relevant landmark for the frontal sinus drainage pattern, but it also helps to assess the distance to AEA. However, it should be highlighted that both UAUP and AEA trajectory are variables and cannot serve as landmarks if not properly assessed on multiplanar scans of CT preoperatively. This prevents intraoperative bleeding during surgical dissection. The more superior at the skull base the upper attachment of the uncinate process (UAUP) is, the more likely the bleeding from AEA with iatrogenic CSF leak. Destabilization of both the uncinate process attachment to the connection between the middle turbinate and the lateral lamella of the cribriform plate (type IV) as well as attachment of UP to the skull base (V) increases the risk of CSF leak. Moreover, very high UAUP to the posteromedial wall of Ager nasi cell or lamina papyracea (type II) decreases the distance to AEA and increases the risk of intra-orbital bleeding and postoperative hematoma. The split superior attachment of UP to the lamina papyracea and to the connection with the middle turbinate and LLCP (type III) brings about a twofold higher risk of bleeding from AEA and CSF leak. Thus, we measured distances between UAUP and AEA at the skull base. The results of the measurement alert the surgeon as to whether AEA is away from UAUP, especially when UAUP is attached directly to the skull base (type IV, V) and therefore this area is more susceptible to damage. The thin part of the lateral lamella of the cribriform plate (LLCP) is prone to the impact of the slightest force from surgical manipulations [20]. We argue that the measurement of the distance between AEA and UAUP allows for identification of the most hazardous steps by dissection which takes place in the case of uncinate process type IV (men – 0%, women – 5.88%) and type V (men – 3.85%, women – 8.82%), respectively. The correlation between the type of UAUP i. e. IV-V-VI and the distance AEA-UAUP was significant (p = 0.017). In types IV-V-VI of UAUP, the mean distance was 8 mm and 9 mm on

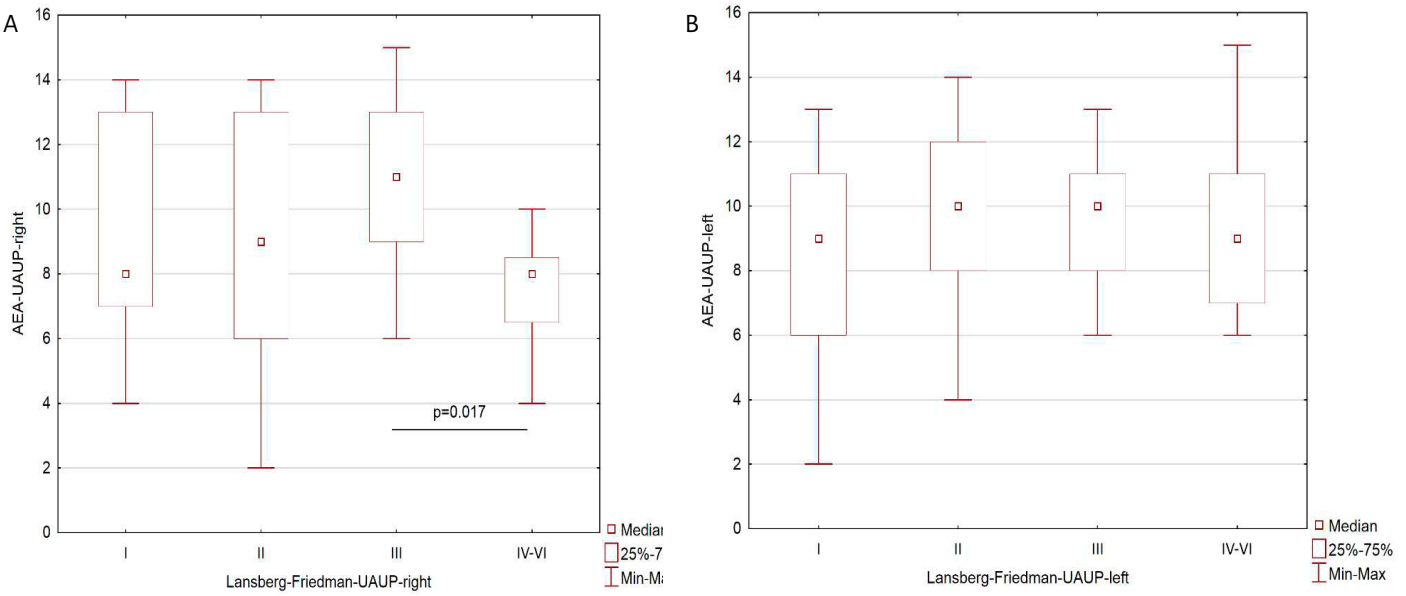

Fig. 3. (A) Relation between the distance AEA-UAUP and the type of uncinete process according to Landsberg-Friedman criteria, right side. (B) Relation between the distance AEA-UAUP and the type of uncinate process according to Landsberg-Friedman criteria left side.

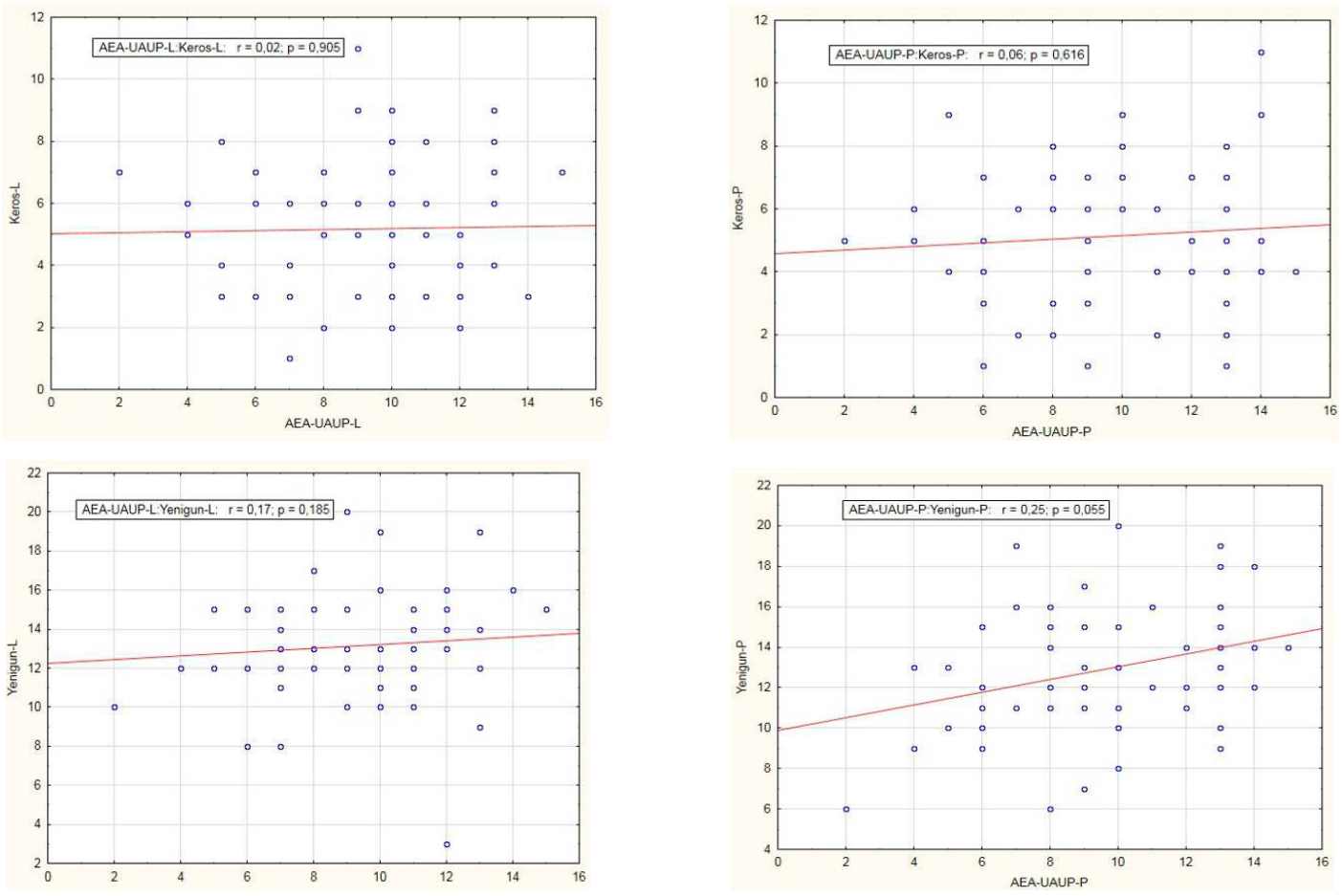

Fig. 4. There is no strong correlation between LLCP length in anterior – posterior dimension (Yenigun criteria) and AEA-UAUP ratio on either side (left side: r = 0,17; p = 0,185, right ride: r = 0,25; p = 0,55). Furthermore, no strong correlation was found between the depth of the LLCP in superior-inferior dimension (Keros criteria) and the AEA-UAUP ratio on either side (left side: r = 0,02; p = 0,905, right side r = 0,06; p = 0,616).The length and slant of the LLCP alone does not significantly determine the AEA-UAUP distance amongst group of patients in the study.In clinical practice it is a relevant information. Thus it indicates that with an increase in length of LLCP and with increase in the depth of the etmoid roof, there is no increase in the risk to intraoperative AEA injury. However, this result does not exclude the risk of iatrogenic CSF leak during surgery. If the LLCP length and deep of the ethmoid roof significantly increases, i.e in anterior skull base configuration type III according to Keros and Yenigun criteria, the risk of iatrogenic CSF leak is the highest.

the right and left side respectively. The distances between UAUP and AEA were estimated in sagittal CT scans. Sagittal reconstructions showed also a bony mesentery connecting AEAs with the fovea ethmoidalis, which is in accordance with the studies by Ferrari et al. [16] and Kainz et al. [21]. Moreover, the latter author [21] highlights the presence of bony dehiscence in the AEA canal in up to 40% of cases. Dehiscence within the bony canal of AEA plays a pivotal role in spreading intracranial or orbital complications observed in rhinosinusitis and intraoperative injuries of an artery.

Proper preoperative imaging technique, as well as surgical devices influence the efficacy of frontal sinus surgery. Narrow space around the frontal recess and assessment of intra-frontal lesions demand proper instrumentations. As Bolzoni Villaret et al. [22] suggest, to reduce soft tissue manipulations and postoperative stenosis, ultrasound bone curette is considered as an effective tool for frontal sinus osteoma removal. Unsuitable armamentarium of surgical tools may lead to parietal mucosa damage and excavation of bony surfaces in the vicinity of a natural frontal ostium which results in stenosis during postoperative recovery time. Moreover, the alleged causes of frontal sinus obstruction and frequent revision surgeries are incomplete anterior ethmoidectomies (in up to 64% of cases), unremoved frontal recess cells (in up to 11.9%) [23] and ager nasi cells in 49% of cases [23]. To decrease the percentage of complications, it is required to conduct a thorough preoperative evaluation of multiplanar reconstructions of CT scans, which are the gold standard in radiological evaluation.

Multiplanar reconstructions of CT images (i.e. sagittal, coronal, axial) complement each other and yield detailed anatomical information [5]. Axial CT scans alone do not reveal bony, rudimentary clefts which remain and narrow the patency of the frontal sinus. According to Wright et al. [24], the coronal plane of CT reflexes the endoscopic view of the surgeon from the anterior to the posterior perspective. Also Minni et al. [18] underline that CT multiplanar reconstructions allow for an adequate evaluation of frontal sinus pathologies. However, this is the sagittal plane that visualizes the frontal recess anatomy the best. According to Kho et al. [25], the axial planes of CT allow for proper identification of three ethmoid arteries (AET, MEA, PEA), while the sagittal planes allow for measurement of distances between structures e.g. posterior ethmoid artery (PEA) and anterior sphenoid wall or optic canal. As in the study by Kho et al. [25], our measurements of the distance between UAUP and AEA were made on sagittal scans. The smallest distance between UAUP and AEA was 2 mm and the longest reached 15 mm on both sides; 9.16 mm (left) and 9.73 mm (right) on average. According to Simmen et al. [15], the distance between AEA and the posterior wall of the frontal recess was about 11 mm (range from 6 to 15 mm), but the upper attachment of the uncinate process is located more anteriorly than the posterior wall of the frontal sinus. This explains why our results differ from those reported by Simmen et al. [15]. Reduction in the distance between UAUP and AEA causes the risk of intraoperative bleeding when approaching the frontal recess. The assessment of the UAUP-AEA distance is clinically relevant to a laryngologist when deciding on frontal sinus surgery.

According to Kainz et al. [21], the most hazardous configuration of the anterior skull base (Keros type III), i.e. the so called "dangerous roof", is when the cribriform plate is roughly 8–16 mm below the ethmoid roof. The thickness of LLCP is less than 0.2 mm and it may be reduced to 0.05 mm at the point where AEA transfixes the latter and enters the olfactory fossa [6]. Yenigun et al. [8] point out that increased superior-inferior depth (Keros criteria) and anterior-posterior length of LLCP, with concomitant supraorbital pneumatization, affects the position of AEA which is exposed below the skull base. Abdullah et al. [20] highlight that the position of AEA at the skull base is not only influenced by the presence of supraorbital cells but also by the length of LLCP. This anatomical variability poses an intraoperative risk of injury of AEA. In the case of decreased anterior-posterior length of LLCP, AEA more frequently emerges at or within the skull base and is less prone to injury. This statement is in accordance with Keros criteria. According to Yenigun and Keros criteria [8, 7], decreased depth of the ethmoid roof (superior-inferior dimension of LLCP) is correlated with the AEA position within the skull base. In brief, White et al. [24] allege that AEA passes forward from the ethmoid roof in the posterior-inferior direction, toward the ethmoidal sulcus in LLCP. Thus, both the anterior-posterior length and the superior-inferior depth of LLCP provide a relevant three-dimensional (3-D) description. Moreover, Munoz-Leila et al. [26] stress that both the Keros and Yenigun criteria may be used for risk assessment. Anterior cranial fossa configuration and its correlation with the trajectory of AEA and UAUP are issues to be considered in radiological imaging before surgical approach to the region of the ethmoid and frontal sinuses. The disadvantage of our study is the lack of evidence from pneumatization assessment in the region of the ethmoid and skull base. However, our aim was to assert the clinical relevance of Keros and Yenigun criteria and correlation between UAUP and AEA.

CONCLUSIONS

UAUP is of great value as a landmark guiding both the laryngologist and the radiologist to discern frontal sinus drainage; it also reveals dangerous relations in anterior skull base configuration. Thorough assessment of the correlation between LLCP and the trajectory of UAUP, prevents inadvertent damage to AEA and CSF leak, especially in type IV and V according to Landsberg-Friedman criteria of the uncinate process. In the present study group type IV-V-VI of UP correlated with a short distance from AEA i.e. range from 4 to 10 mm, mean value: 8 mm ($p = 0.017$). Hence, the measurement of the distance between UAUP and AEA is regarded as congruent.

Also, the configuration of the anterior skull base according to both Keros and Yenigun criteria is considered to be relevant as it shows the 3D configuration of the examined area.

AEA may also serve as a reference in clinical practice, as its branches transverse the region of the posterior wall of the frontal sinus, especially medially in the anterior ethmoidal roof. However, because of its variability, preoperative CT multiplanar reconstructions are mandatory.

1. Preoperative identification of AEA, UAUP and configuration of the anterior skull base in multiplanar reconstructions of CT is the factor necessary for obtaining optimal results of frontal sinus surgery;
2. There is a correlation between the type of the uncinate process and the distance between UAUP and AEA. According to Landsberg-Friedman criteria, types IV-V-VI of the uncinate process contribute to a decrease in the UAUP-AEA distance and to an increase in the risk of AEA injury;
3. Keros and Yenigun criteria are the same for anterior skull base configuration; however, if used together, they complement each other and yield 3-D configuration. In our results, the most frequent type II according to Keros was compatible with type II according to Yenigun.

REFERENCES

1. Turgut S., Ercan I., Sayin I., Basak M.: The relationship between frontal sinusitis and localization of the frontal sinus outflow tract. A computed-assisted anatomical and clinical study. Arch Otolaryngol Head Neck Surg, 2005; 5: 518–522.
2. Leunig A.: Endoscopic surgery of the lateral nasal wall, paranasal sinuses and anterior skull base. 2014 Endo: Press, Tuttlingen: 46–47.
3. Messerklinger W.: On the drainage of the normal frontal sinuses of man. Acta Otolaryngol (Stockh), 1967; 63: 176–181.
4. Stammberger H., Hawke M.: Functional Endoscopic Sinus Surgery. Philadelphia. Pa: BC Decker Publishers: 1991.
5. Leunig A., Sommer B., Betz C.S., Sommer F.: Surgical anatomy of the frontal recess-is there a benefit in multiplanar – CT reconstructions? Rhinology, 2008; 46: 188–194.
6. Stammberger H., Lund V.J.: Anatomy of the nose and paranasal sinuses. In: Scott-Brown's Otorhinolaryngology: head and neck surgery, Ed.: M. Gleeson, G.G. Browning, M.J. Burton et al., 7th Edition Hodder Arnold, London 2008: 1335.
7. Keros P.: On the practical value of differences in the level of the lamina cribrosa of the ethmoid. Z Laryngol Rhinol Otol, 1962; 41: 809–813.
8. Yenigun A., Goktas S.S., Dogan R., Eren S.B., Ozturan O.: A study of the anterior ethmoidal artery and a new classification of the ethmoid roof (Yenigun classification). Eur. Arch. Otorhinolaryngol, 2016; 273: 3759–3764.
9. Landsberg R., Friedman M.: A computer-assisted anatomical study of the nasofrontal region. Laryngoscope, 2001; 111: 2125–2130.
10. De Bonnecaze G., Gallois Y., Chaynes P., Bonneville F., Dupret-Bories A. et al.: Intractable epistaxis: which arteries are responsible? An angiographic study. Surg. Radiol. Anat., 2017; 39; 11: 1203–1207.
11. Bischoff S., Gerth-Kahlert C., Holzmann D., Soyka M.B.: Longstanding diplopia after ethmoidal artery ligation for epistaxis. Eur. Arch. Otorhinolaryngol., 2020; 277: 161–167.
12. Turri-Zanoni M., Arosio A.D., Stamm A.C., Battaglia P., Salzano G. et al.: Septal branches of the anterior ethmoidal artery: anatomical considerations and clinical implications in the management of refractory epistaxis. Eur. Arch. Otorhinolaryngol, 2018; 275: 1449–1456.
13. Sokoloff J., Wickbom I., McDonald D., Brahme F., Goergen T.C.: Therapeutic percutaneous embolization in intractable epistaxis. Radiology, 1974; 2: 285–287.
14. Moon H.J., Kim H.U., Lee J.G., Chung I.H., Yoon J.H.: Surgical Anatomy of the anterior ethmoidal canal in ethmoid roof. Laryngoscope, 2001; 111; 5: 900–904.
15. Simmen D., Raghavan U., Briner H.R., Manestar M., Schucknecht B. et al.: The surgeon's view of the anterior ethmoid artery. Clin. Otolaryngol., 2006; 31: 187–191.
16. Ferrari M., Pianta L., Borghesi A., Schreiber A., Ravanelli M. et al.: The ethmoidal arteries: a cadaveric study based on cone beam computed tomography and endoscopic dissection. Surg. Radiol. Anat., 2017; 39: 991–998.
17. Stammberger H., Posawetz W.: Functional endoscopic sinus surgery. Concept, indications and results of Messerklinger technique. Eur Arch Otorhinolaryngol, 1990; 247: 63–76.
18. Minni A., Messineo D., Attanasio G., Pianura E., D'Ambrosio F.: 3-D cone beam (CBCT) in evaluation of frontal recess: findings in youth population. Eur Rev Med Pharmacol Sci, 2012; 16: 912–918.
19. Stammberger H.: "Uncapping the Egg" 1995 at the "3rd International Symposium on Advanced FESS" at Cairns/Australia 1995.
20. Abdullah B., Lim E.H., Husain S., Snidvongs K., Wang D.Y.: Anatomical variations of anterior ethmoidal artery and their significance in endoscopic sinus surgery: a systematic review. Surg. Radiol. Anat., 2019; 41: 491–499.
21. Kainz J., Stammberger H.: The roof of the anterior ethmoid: a locus minoris resistentiae in the skull base. Laryngol Rhinol Otol (Stutt), 1988; 67(4): 142–149.
22. Bolzoni Villaret A., Schreiber A., Esposito I., Nicolai P.: Endoscopic ultrasonic curette-assisted removal of frontal osteomas. Acta Otorhonolaryngo, 2014; 34: 205–208.
23. Chiu A.G., Vaughan W.C.: Revision endoscopic frontal sinus surgery with surgical navigation. Otolaryngol Head Neck Surg, 2004; 130: 312–318.
24. White D.V., Sincoff E.H., Abdulrauf S.I.: Anterior ethmoidal artery: microsurgical anatomy and technical considerations. Neurosurgery, 2005; 56(2 Suppl): 406–410.
25. Kho J.P., Tang I.P., Tan K.S., Koa A.J., Prepageran N. et al.: Radiological study of the ethmoidal arteries in the nasal cavity and its pertinence to the endoscopic surgeon. Indian J Otolaryngol Head Neck Surg, 2019; 71(Suppl3): 1994–1999.
26. Munoz-Leila M.A., Yamamoto-Ramos M., Barrera-Flores F.J., Trevino-Gonzales J.L., Quiroga-Garza A. et al.: Anatomical variations of the ethmoidal roof: differences between men and women. Eur. Arch. Otorhinolaryngol., 2018; 275: 1831–1836.

Word count: 3676 Page count: 8 Tables: 5 Figures: 4 References: 26

DOI: 10.5604/01.3001.0014.2471 Table of content: https://ppch.pl/issue/13341

Competing interests: The authors declare that they have no competing interests.

Corresponding author: Greta Berger; TMS Diagnostyka, Bialystok, Poland; E-mail: greta.ewa.berger@gmail.com

Cite this article as: Berger G., Grinevych V., Milewska A.J., Lukasiewicz A., Tarasow E.: Estimation of ethmoid roof depth and length of lateral lamella of the cribriform plate, upper attachment of the uncinate process and anterior ethmoid artery in multiplanar reconstructions of Computed Tomography; Pol Przegl Chir 2020: 92 (5): 15–23